Research Article | Vol. 26, No. 22 | 29 Oct 2018 | OPTICS EXPRESS 28621
Optics EXPRESS

Laser frequency stabilization and spectroscopy at 2051 nm using a compact CO_2-filled Kagome hollow core fiber gas-cell system

E. Anne Curtis,[1,*] Thomas Bradley,[2] Geoffrey P. Barwood,[1] Christopher S. Edwards,[1] Natalie V. Wheeler,[2] Richard Phelan,[3] David J. Richardson,[2] Marco N. Petrovich,[2] and Patrick Gill[1]

[1]*National Physical Laboratory, Hampton Road, Teddington, TW11 0LW, UK*
[2]*Optoelectronics Research Centre, University of Southampton, Highfield, Southampton, Hampshire, SO17 1BJ, UK*
[3]*Eblana Photonics Ltd, 3 West Pier Business Campus, Dun Laoghaire, Co. Dublin, A96 A621, Ireland*
[*]*anne.curtis@npl.co.uk*

Abstract: We describe a compact, all fiber, frequency stabilized diode laser system at 2051 nm using CO_2 gas-filled Kagome Hollow Core Fiber (HCF), capable of tuning continuously over four transitions in $^{12}C^{16}O_2$: R(24), R(26), R(28), and R(30). This laser system has been designed for use in future space-based atmospheric monitoring using differential absorption lidar (DIAL). The fully spliced Kagome HCF gas cell is filled to 2 kPa CO_2 partial pressure and we compare the observed CO_2 lineshape features with those calculated using HITRAN, to quantify the properties of the CO_2-filled fiber cell. In this first demonstration of Kagome HCF used in a fully sealed gas cell configuration for spectroscopy at 2 μm, we characterize the frequency stability of the locked system by beat frequency comparison against a reference laser. Results are presented for the laser locked to the center of the $^{12}C^{16}O_2$ R(30) transition, with frequency stability of ~40 kHz or better at 1 s, and a frequency reproducibility at the 0.4-MHz level over a period of > 1 month. For DIAL applications, we also demonstrate two methods of stabilizing the laser frequency ~3 GHz from this line. Furthermore, no pressure degradation was observed during the ~15-month period in which frequency stability measurements were acquired.

OCIS codes: (300.6390) Spectroscopy, molecular; (300.6380) Spectroscopy, modulation; (060.4005) Microstructured fibers; (140.3425) Laser stabilization; (280.1910) DIAL, differential absorption lidar.

References and links

1. K. W. Rothe, U. Brinkman, and H. Walter, "Applications of tunable dye lasers to air pollution detection: Measurements of atmospheric NO_2 concentrations by differential absorption," Applied Physics **3**, 115–119 (1974).
2. R. A. Robinson, T. D. Gardiner, F. Innocenti, A. Finlayson, P. T. Woods, and J. F. M. Few, "First Measurements of a Carbon Dioxide Plume from an Industrial Source Using a Ground Based Mobile Differential Absorption Lidar," Environmental Science: Processes & Impacts **16**, 1957–1966 (2014).
3. IPCC, 2014: Climate Change 2014: Synthesis Report. Contribution of Working Groups I, II and III to the Fifth Assessment Report of the Intergovernmental Panel on Climate Change [Core Writing Team, R.K. Pachauri and L.A. Meyer (eds.)]. IPCC, Geneva, Switzerland, 151 pp.
4. "A-SCOPE–Advanced Space Carbon and Climate Observation of Planet Earth, Report For Assessment," ESA-SP1313/1 (European Space Agency, 2008). http://esamultimedia.esa.int/docs/SP1313-1_ASCOPE.pdf
5. J. Barrientos Barria, D. Mammez, E. Cadiou, J. B. Dherbecourt, M. Raybaut, T. Schmid, A. Bresson, J. M. Melkonian, A. Godard, J. Pelon, and M. Lefebvre, "Multispecies high-energy emitter for CO_2, CH_4 and H_2O monitoring in the 2 μm range," Optics Letters **39**, 6719–6722 (2014).
6. R. T. Menzies and D. M. Tratt, "Differential laser absorption spectrometry for global profiling of tropospheric carbon dioxide: selection of optimum sounding frequencies for high-precision measurements," Applied Optics **42**, 6569–6577 (2003).

#338573 https://doi.org/10.1364/OE.26.028621
Journal © 2018 Received 27 Jul 2018; revised 13 Sep 2018; accepted 18 Sep 2018; published 19 Oct 2018

Optics EXPRESS

7. G. D. Spiers, R. T. Menzies, J. Jacob, L. E. Christensen, M. W. Phillips, Y. Choi, and E. V. Browell, "Atmospheric CO_2 measurements with a 2 μm airborne laser absorption spectrometer employing coherent detection," Applied Optics **50**, 2098–2111 (2011).
8. J. Caron and Y. Durand, "Operating wavelengths optimization for a spaceborne lidar measuring atmospheric CO_2," Applied Optics **48**, 5413–5422 (2009).
9. P. Meras, I. Y. Poberezhskiy, D. H. Chang, and G. D. Spiers, "Frequency Stablization of a 2.05 μm Laser Using Hollow-Core Fiber CO_2 Frequency Reference Cell," Proc. SPIE **7677**, 767713–767713-9 (2010).
10. P. G. Westergaard, J. W. Thomsen, M. R. Henriksen, M. Michieletto, M. Triches, J. K. Lyngsø, and J. Hald, "Compact, CO_2-stabilized tuneable laser at 2.05 microns," Optics Express **24**, 4872–4880 (2016).
11. J. W. Nicholson, L. Meng, J. M. Fini, R. S. Windeler, A. DeSantolo, E. Monberg, F. DiMarcello, Y. Dulashko, M. Hassan, and R. Ortiz, "Measuring higher-order modes in a low-loss, hollow-core, photonic-bandgap fiber," Optics Express **20**, 20494–20505 (2012).
12. T. D. Bradley, N. V. Wheeler, G. T. Jasion, D. Grey, J. Hayes, M. A. Gouveia, S. R. Sandoghchi, Y. Chen, F. Poletti, D. Richardson, and M. N. Petrovich, "Modal content in hypocycloid Kagomé hollow core photonic crystal fibers," Optics Express **24**, 104–113 (2016).
13. J. Tuominen, T. Ritari, H. Ludvigsen, and J. C. Petersen, "Gas filled photonic bandgap fibers as wavelength references," Optics Communications **255**, 272–277 (2005).
14. J. Henningsen, J. Hald, and J. C. Petersen, "Saturated absorption in acetylene and hydrogen cyanide in hollow-core photonic bandgap fibers," Optics Express **13**, 10475–10482 (2005).
15. A. Lurie, F. N. Baynes, J. D. Anstie, P. S. Light, F. Benabid, T. M. Stace, and A. N. Luiten, "High-performance iodine fiber frequency standard," Optics Letters **36**, 4776–4778 (2011).
16. K. Knabe, S. Wu, J. Lim, K. A. Tillman, P. S. Light, F. Couny, N. Wheeler, R. Thapa, A. M. Jones, J. W. Nicholson, B. R. Washburn, F. Benabid, and K. L. Corwin, "10 kHz accuracy of an optical frequency reference based on $^{12}C_2H_2$-filled large-core kagome photonic crystal fibers," Optics Letters **17**, 16017–16026 (2009).
17. N. V. Wheeler, "Molecular and Atomic Confinement in Large Core Photonic Microcells for Slow Light and Laser Metrology Applications," PhD Thesis, University of Bath, (2010).
18. F. Benabid, F. Couny, J. C. Knight, T. A. Birks, and P. St J. Russell, "Compact, stable and efficient all-fibre gas cells using hollow-core photonic crystal fibres," Nature **434**, 488–491 (2005).
19. G. C. Bjorklund, "Frequency modulation spectroscopy: a new method for measuring weak absorptions and dispersions," Optics Letters **5**, 15–17 (1980).
20. R. Phelan, J. O'Carroll, D. Byrne, C. Herbert, J. Somers, and B. Kelly, "$In_{0.75}Ga_{0.25}As$/InP Multiple Quantum-Well Discrete-Mode Laser Diode Emitting at 2 μm," IEEE Photonics Technology Letters **24**, 652–654 (2012).
21. I. E. Gordon, L. S. Rothman, C. Hill, R. V. Kochanov, Y. Tan, P. F. Bernath, M. Birk, V. Boudon, A. Campargue, K. V. Chance, B. J. Drouin, J.-M. Flaud, R. R. Gamache, J. T. Hodges, D. Jacquemart, V. I. Perevalov, A. Perrin, K. P. Shine, M.-A. H. Smith, J. Tennyson, G. C. Toon, H. Tran, V. G. Tyuterev, A. Barbe, A. G. Császár, V. M. Devi, T. Furtenbacher, J. J. Harrison, J.-M. Hartmann, A. Jolly, T. J. Johnson, T. Karman, I. Kleiner, A. A. Kyuberis, J. Loos, O. M. Lyulin, S. T. Massie, S. N. Mikhailenko, N. Moazzen-Ahmadi, H. S. P. Müller, O. V. Naumenko, A. V. Nikitin, O. L. Polyansky, M. Rey, M. Rotger, S. W. Sharpe, K. Sung, E. Starikova, S. A. Tashkun, J. Vander Auwera, G. Wagner, J. Wilzewski, P. Wcisło, S. Yu, and E. J. Zak, "The HITRAN2016 molecular spectroscopic database," Journal of Quantitative Spectroscopy & Radiative Transfer, **203**, 3-69 (2017).
22. J. Wang, P. Ehlers, I. Silander, and O. Axner, "On the accuracy of the assessment of molecular concentration and spectroscopic parameters by frequency modulation spectrometry and NICE-OHMS," Journal of Quantitative Spectroscopy & Radiative Transfer **136**, 28–44 (2014).
23. F. Poletti, M. N. Petrovich, and D. J. Richardson, "Hollow-core photonic bandgap fibers: technology and applications," Nanophotonics **2**, 315–340 (2013).
24. N. Wilding, P. S. Light, F. Couny, and F. Benabid, "Experimental Comparison of Electromagnetically Induced Transparency in Acetylene-Filled Kagome and Triangular Lattice Hollow Core Photonic Crystal Fiber." In 2008 Conference on Lasers and Electro-Optics & Quantum Electronics and Laser Science Conference, Vol. 1-9, 1953-1954, IEEE Lasers and Electro-Optics Society (LEOS) Annual Meeting (2008).
25. N. V. Wheeler, T. D. Bradley, J. R. Hayes, M. A. Gouveia, S. Liang, Y. Chen, S. R. Sandoghchi, M. S. Abokhamis, F. Poletti, M. N. Petrovich, and D. Richardson, "Low-loss Kagome hollow-core fibers operating from the near- to the mid-IR," Optics Letters **42**, 2571–2574 (2017).
26. M. Maurel, M. Chafer, F. Delahaye, F. Amrani, B. Debord, F. Gerome, and F. Benabid "2-μm wavelength-range low-loss inhibited-coupling hollow-core PCF," SPIE Proceedings Volume 10513, Components and Packaging for Laser Systems IV, 10513–10513–6 (2018).
27. P. S. Light, F. Couny, and F. Benabid, "Low optical insertion-loss and vacuum-pressure all-fiber acetylene cell based on hollow-core photonic crystal fiber," Optics Letters **31**, 2538–2540 (2006).
28. E. A. Curtis, G. P. Barwood, G. Huang, C. S. Edwards, B. Gieseking, and P. J. Brewer, "Ultra-high-finesse NICE-OHMS spectroscopy at 1532 nm for calibrated online ammonia detection," Journal of the Optical Society of America B **34**, 950–958 (2017).

Optics EXPRESS

1. Introduction

Global detection and monitoring of atmospheric trace gases, particularly those of specific interest in the study of climate change, require a long-term solution. A space-borne method of active sensing of greenhouse gases would provide such coverage and can be accomplished using differential absorption lidar (DIAL) [1, 2] with either one or a number of satellites in low-earth orbit. DIAL can be configured to sense different greenhouse gases such as methane or carbon dioxide via the use of lasers at different infrared wavelengths. Of the various greenhouse gases currently under long-term observation, the most important is carbon dioxide (CO_2) [3, 4]. Some work on suitable high-power laser sources for DIAL applications has already been published [5]; however, for satellite deployment, an on-board, compact and frequency-stabilized low-power laser system is also required, necessary for seeding this higher power device. With DIAL, a laser is tuned to line center of a strong absorption of CO_2, and then significantly away from the center, and the differential back-scattered light is measured. In earlier studies, the Jet Propulsion Laboratory (JPL) concluded that lines in the 20013-00001 band from $^{12}C^{16}O_2$ at 2 μm were best suited for this application [6]. In their 2009 lidar measurements [7], JPL selected the R(30) line and this was also chosen by ESA for their planned DIAL activities [8]. Whilst earlier studies used conventional free-space cells, more recent work has investigated the use of Hollow Core Fiber (HCF)-based cells, as these offer a potentially more robust and lightweight optical package for space applications. Past studies have published results for laser stabilization to CO_2-filled Hollow Core Photonic Bandgap Fiber (HC-PBGF) [9, 10]. In contrast, the work reported here presents results for Kagome HCF-based cells, looking at long-term stability as well as investigating different options for off-resonant frequency stabilization. We focus on using Kagome HCFs for fully spliced fiber gas cells because of the ability to fabricate fibers with large core diameters to decrease gas filling times whilst maintaining low loss and low bend loss with the added advantage of reduced multimode interference as compared to HC-PBGFs [11, 12].

It was first suggested over 10 years ago that HCFs might be filled with different gases such as acetylene and methane in order to provide frequency references [13]. HCFs provide transverse mode confinement in combination with very long interaction lengths in a hollow core. If the hollow core is then filled with a suitable gas, these HCFs can provide significantly enhanced light-matter interactions in a compact arrangement as compared to traditional gas cells, thus increasing the signal-to-noise ratio (SNR).

Frequency-stabilized laser systems with HCFs have either a low-pressure fill and use saturated (Doppler-free) spectroscopy or a higher pressure fill and use linear absorption. Doppler-free spectroscopy gives much narrower spectral linewidths and consequently better frequency stability (see, for example, [14–16]) but this leads to a more complex optical arrangement. The systems in [14–16] also had the fiber terminated within a vacuum chamber, so were not fully sealed; a re-sealable system has also been developed [17]. However, where ~kHz frequency stability is not routinely required, the most compact and transportable arrangement will employ Doppler- or pressure-broadened linear spectroscopy in a permanently sealed fiber [10, 18]. The scope of the work presented here is to demonstrate DIAL-compatible frequency stability in a compact, all-fiber gas cell that is free from cumbersome vacuum technology.

For this space-based DIAL application, the target frequency stability (Allan deviation) is 100 kHz at 10 s [4]. In the following sections we discuss both our HCF frequency reference system, which uses Pound-Drever-Hall (PDH) spectroscopy [19] for laser stabilization, and our reference laser system, which is used to probe the stability of the HCF system. This reference uses wavelength modulation spectroscopy as a basis for frequency stabilization, observing CO_2 features in a conventional sealed and commercially-sourced low-pressure cell. We demonstrate the reproducibility and stability of our fiber-based system by beat frequency comparison between these two systems.

Optics EXPRESS

2. Laser spectroscopy

The Eblana InP DFB laser [20] used for this work had a continuous tuning range of more than 150 GHz (>5 cm^{-1}) at 2051 nm, and a measured linewidth of 2 MHz half-width at half maximum (HWHM). It was therefore possible to access a number of well-resolved linear absorption features with a single laser source, as shown in Fig. 1. Strong lines from both the principal isotopologue

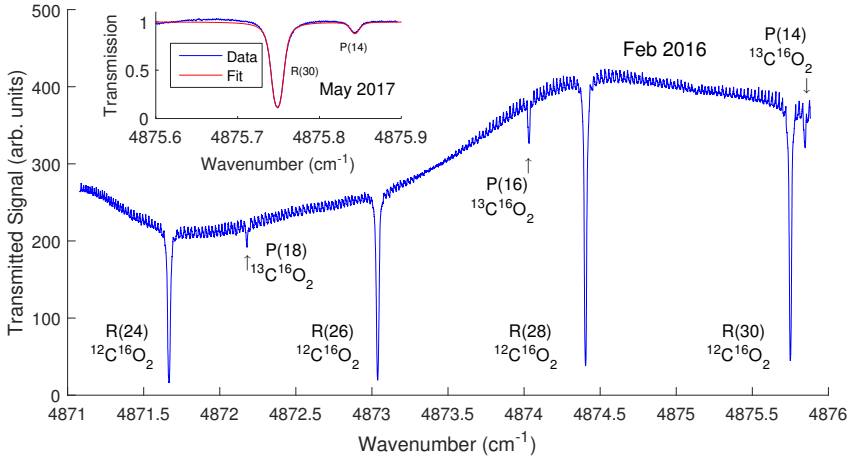

Fig. 1. Main figure: (Data from February 2016) A 5-cm^{-1} (~150-GHz) scan over four strong features in the vicinity of R(30) for a 5-m long, fully spliced Kagome HCF cell filled with 2 kPa of CO_2. The weaker lines have approximately 5 % of the linear absorption of the stronger lines. The scan was taken by temperature tuning of the laser. This gives rise to a small linear change of power with frequency, but the baseline changes mainly arise from frequency-dependent transmission variations in the fiber cell. Inset: data from a short-range, 0.3 cm^{-1} (~9 GHz) scan (produced by laser current tuning) taken in May 2017 over the $^{12}C^{16}O_2$ R(30) and $^{13}C^{16}O_2$ P(14) transitions; the result can be compared with the R(30) and P(14) features in the main figure, which were taken using the same fiber cell 15 months prior. At these times, the peak absorption of the main feature was measured as 87(5) % (Feb 16) and 92(5) % (May 17), the same to within the experimental uncertainty. A total pressure is estimated from the fit (linear background subtracted), consistent with the targeted 2 kPa partial pressure. The reduction of baseline noise between the two measurements is also due to a change in the fiber configuration between measurements.

$^{12}C^{16}O_2$ and weaker lines from $^{13}C^{16}O_2$ can be observed; the line strengths and center frequencies are listed in HITRAN2016 [21]. According to HITRAN, the $^{12}C^{16}O_2$ and $^{13}C^{16}O_2$ lines arise from the 20013 - 00001 and 20012 - 00001 bands, respectively. The linear absorption profile is straightforward to model as the complex Faddeeva function [22]; the real part of this function is the familiar Voigt profile. Here the complex parameter z is given by:

$$z = \frac{(\nu - \nu_0)}{\Gamma_D} + i\frac{\Gamma_L}{\Gamma_D} \tag{1}$$

The Doppler and Lorentzian HWHM linewidths are Γ_D and Γ_L, respectively; ν_0 denotes line center. For CO_2, Γ_D = 0.0047 cm^{-1} (≡ 140 MHz). The cross section profile is normalized so that for a single spectral component, integrating this cross section over all frequencies ν yields the line strength S.

For a set of molecular transitions $\{j\}$, the total linear absorbance A over a path length L is

Optics EXPRESS

given by:

$$A = NL \sum_j S_j V_j(\nu) \tag{2}$$

Here, N denotes the number of absorbing (CO_2) molecules per unit volume, L the HCF cell length and V the normalized Voigt profile. The transmitted signal (T) is given by:

$$T \propto \exp(-A) \tag{3}$$

Typically, absorption lines from the same isotopologue in this spectral region are 1.3 cm^{-1} (≡ 40 GHz) apart in frequency. One advantage of the R(30) transition is that there is a weak line due to $^{13}C^{16}O_2$ only ~2.8 GHz higher in frequency, within the measurement range of commercially-available detectors and counters. Our arrangement for comparing two CO_2-frequency stabilized lasers is shown in Fig. 2. With both lasers stabilized to the R(30) CO_2 absorption line, the beat between them is predominantly determined by the 80-MHz drive frequency of the acousto-optic modulator offsetting the reference frequency by that amount. If the HCF system is instead locked to the weak $^{13}C^{16}O_2$ line, then a beat of ~2.8 GHz is recorded (see section 6).

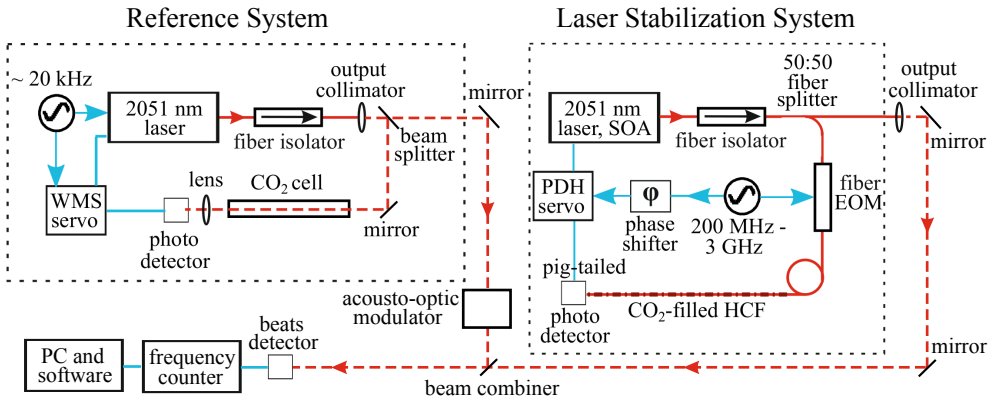

Fig. 2. Experimental layout for the frequency stabilized laser systems using fully spliced CO_2-filled Kagome HCF and a free-space cell. Fiber links are indicated by solid red lines; free space beams are dashed and blue lines are electronic connections: SOA (semiconductor optical amplifier), WMS (wavelength modulation spectroscopy), PDH (Pound-Drever-Hall), EOM (electro-optic modulator). Optical outputs from both systems were combined on a beam combiner and focused onto a free-space photo diode (beats detector) with ~12-GHz bandwidth. The resulting beat frequency was monitored and recorded using a frequency counter coupled to a computer with GPIB interface.

In addition to line-strengths and center frequencies, HITRAN lists coefficients for pressure broadening due either to CO_2 or air. For R(30), the air broadening HWHM is 0.069 cm^{-1}/atm and the self-broadening is 0.090 cm^{-1}/atm. At low pressures, where Doppler broadening dominates, the normalized absorption profile is independent of pressure and the peak absorption increases with number density and therefore pressure [Eq. (2)]. At high pressures, where pressure broadening dominates, the absorption at line center is independent of pressure but the linewidth increases. We therefore expect that optimum frequency stability should be achieved when maximizing signal size and minimizing linewidth, which occurs when the pressure broadening does not contribute as significantly as the Doppler component. For self-pressure broadening, this limit is ~5 kPa; we should also ensure that any background gas is below ~7 kPa. Our free-space cell is filled to a

Optics EXPRESS

pressure of ~2.6 kPa and, as described in the next section, we set a maximum design pressure for our fibers of ~2 kPa.

A key requirement of fiber-based gas filled cells for laser locking is that the fiber should have a flat spectral transmission in the wavelength region of interest. This is quite challenging in the case of HCFs, as most fiber designs that enable low-loss transmission (and hence a long interaction length) typically support a few transverse optical modes [23]. When a fraction of light is coupled to higher order modes, e.g. due to modal mismatch at the launch and/or collection end, or due to small imperfections or structural deformations at the splice between the HCF and the solid counterpart, modal interference may arise. This will give rise to background signals that can change with environmental conditions and can easily affect the spectroscopic locking technique for the laser stabilization. This can be particularly relevant in the case of very weak or very narrow gas absorption features. It has been previously reported [24, 25] that Kagome HCFs offer significant advantage over other HCF types in this respect. We compared the Kagome HCF-based cells with similar cells based on Hollow Core Photonic Bandgap Fibers (the other most common type of HCF) and verified that their performance was significantly better in terms of spectral flatness on wavelength scales relevant for the observation of gas absorption lines relevant for this study.

3. Fiber fabrication and characterization

A 7-cell Kagome HCF was fabricated through a stack and draw process. The fiber design was chosen as a trade-off between different requirements, including rapid gas filling (due to large core diameter), low transmission and low bending loss, and broad transmission bandwidth covering the target CO_2 transition at 2051 nm [26]. The fabricated Kagome HCF was operated at a wavelength of ~2 μm in its fundamental transmission band [25]. Standard fusion splicing of Kagome fiber is challenging due to the cross sectional scale of the Kagome HCF being typically 2-3 times larger than that of single mode fiber (SMF), and with a very substantial (>205-μm diameter) hollow core and microstructured region at its center, as shown in Fig. 3(a). To mitigate this we adopted a custom designed buffer fiber in order to integrate the HCF into our all-fiber system, as described below. The fabricated fiber has a core formed via seven missing elements at the center of a hexagonal lattice of holes [see optical micrograph in Fig. 3(a)], measuring approximately 55 μm in diameter and with a mode field diameter (MFD) of ~39 μm. The average thickness of the glass struts of the microstructure cladding is ~800 nm; the outer diameter (OD) of the drawn fiber is 340 μm. The thickness and shape of the core surround was optimized for low-loss and quasi-single-mode operation around 2 μm [12, 25]. The black trace in Fig. 3(b) shows the transmission spectrum when a broadband source is launched through a 5-m length of Kagome HCF. The green trace in Fig. 3(b) is the loss measured (cutback technique), demonstrating a minimum value of ~68 dB/km at 1985 nm. The observed fiber transmission bandwidth spans from 1.7 to beyond 2.4 μm, limited by the spectral range of the optical spectrum analyzer used in the measurement presented here.

4. Gas cell fabrication

The large core diameter in our Kagome HCF, although beneficial for gas volume, means that low-loss interconnection of Kagome HCFs with standard SMF can be very challenging due to large mode field mismatch. Furthermore, the larger microstructured region leads to a larger overall OD of the fiber, in this case ~340 μm, which makes it challenging to integrate the HCF cell to standard fiber (typical OD ~125 μm) via fusion splicing.

Prior to fabricating the fiber-based gas cell, two solid fiber pigtails are prepared using a conventional fusion splicer. The pigtails consist of a segment of standard SMF, in this case SMF28, spliced to a short length (~500 mm) of a custom-designed large mode area single mode fiber (LMA SMF) with a MFD ~20 μm. The insertion loss of such a fiber assembly (largely due

Optics EXPRESS

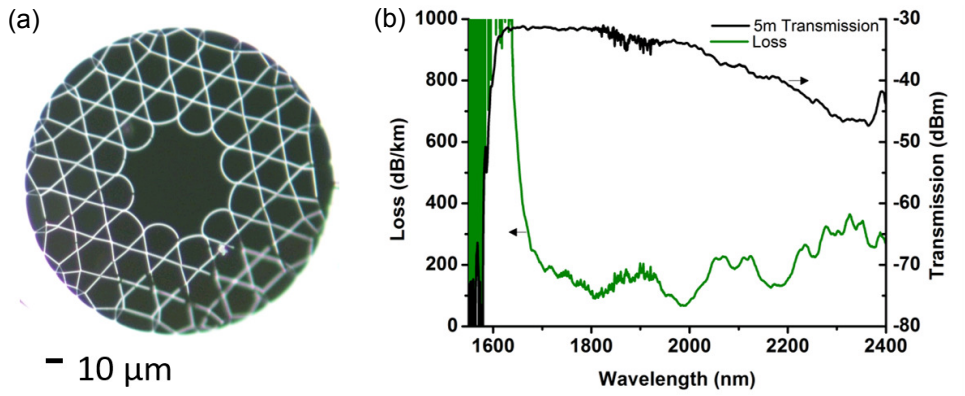

Fig. 3. (a) Optical micrograph showing the microstructure of the Kagome HCF. The fiber has a core composed of seven missing elements and three full rings of large holes surrounding it. The thickness of the core surround is approximately 0.8 µm and the negative curvature design contributes to achieving low transmission loss. (b) Transmission spectrum (black trace) through 5 m of Kagome HCF when a broadband source is launched with solid large mode area single mode fiber. Loss of a comparable Kagome HCF measured by cutback from 51 m to 5 m (green trace).

to the modal mismatch between the standard and the LMA SMF) is ~1.5 dB. The LMA SMF has a larger OD (~250 µm) to enable fusion splicing to the Kagome HCF (MFD ~39 µm and OD ~340 µm) to be performed with high mechanical strength and without adversely impacting the structure of the Kagome HCF. One end of a 5.0-m length of the Kagome HCF was initially spliced to an LMA SMF pigtail, leaving the other end open for the gas filling. The open end was then inserted into a vacuum chamber and pumped down to a base pressure of 4 x 10^{-4} mbar for a period of 48 hours while heating the Kagome HCF to about 100 °C in order to fully evacuate and remove any atmospheric gas species present within the hollow core. Once this process had been completed, the fiber was filled to ~100 kPa (atmospheric pressure) with a calibrated mixture of 2 % CO_2 in helium (2 kPa CO_2 partial pressure), following a comparable technique for an HCF-based acetylene reference [27]. The CO_2 used in our fibers was of a natural isotopic mix, rather than the separate isotopically enhanced samples used in reference [10]. Fill process timing was found to be critical to the success of this fill. If this fiber was left connected to the vacuum chamber containing the helium/CO_2 mixture for too long (e.g. many hours), there was significant diffusion of helium from the fiber, allowing buildup of excess CO_2 in the Kagome HCF. In order to ensure filling of the hollow core to the required CO_2 concentration, the fiber was allowed to fill and stabilize only for approximately 30 minutes. The fiber was then disconnected from the filling system, cleaved, and quickly (~1 minute) spliced to another LMA SMF pigtail. The helium gas present within the sealed fiber cell then diffused through the silica of the Kagome HCF at room temperature. The transmission properties of the fully connectorized fiber gas cell were then measured with a 2-µm Tm-doped fiber amplified spontaneous emission (ASE) source and optical spectrum analyzer to confirm the presence of the CO_2 gas at the target concentration/partial pressure in the hollow core. The sealed gas fiber cell had an insertion loss ~8.5 dB at 2 µm, dominated by modal mismatch between the various fiber segments. When measured soon after filling, the CO_2 features were barely observable. However within ~24 hours, the helium diffused away significantly and the pressure broadening of the CO_2 feature reduced. After ~3 days, the feature had close to the expected absorption strength. The amount of CO_2 and the presence of air was inferred by fitting the observed profiles and comparing to listed HITRAN values, see Fig. 1,

Optics EXPRESS

inset.

5. Long-term stability of Kagome HCF gas cells

HCF gas cells are desirable because of the increased interaction length between the light and the gas confined in the hollow core. The shape and peak value of the absorption profile, and their stability over time, are of primary importance when quantifying the performance of an HCF gas cell. For instance, it is important to verify that the CO_2 is neither adsorbed onto the fiber walls, nor out-diffuses significantly during the splicing operation. Likewise, it is important to verify that ingress of atmospheric species during the splicing operation is minimized: the presence of such species would increase the base pressure within the cell once the helium has diffused, and would broaden the CO_2 linewidth. It is paramount to ensure that the linewidth and contrast are not degrading over time, e.g. due to ingress of atmospheric gases within the cell post-fabrication. This could happen, for instance, due to an imperfect seal at the splice point, or due to the splice itself weakening and failing over time.

It is relatively straightforward to calculate limits to the acceptable leak rates from the HITRAN air-broadening coefficient. Similarly, rates of acceptable adsorption can be estimated. Both adsorption and air ingress will result in a reduction of the linear absorption at line center, as well as broadening the linewidth. The peak linear absorption of the R(30) transition of our 2-kPa fiber cell was measured in February 2016 [Fig. 1] and then in May 2017 [Fig. 1, inset], after a period of over 15 months. From these results, we determined no significant change in the peak absorption; in February 2016, this was measured to be 87(5) % and in May 2017 it was 92(5) %. Comparable stability was observed in several other similarly-produced fiber cells, which suggests our fabrication method is robust and produces gas-filled cells with long lifetimes.

In order to assess and quantify the results of the filling process, the absorption profile was fitted to a Voigt profile [Eqs. (1) and (2)] using routines developed in [28] and the result for the May 2017 linear absorption is shown in the inset to Fig. 1. Before plotting and fitting the results, a small local linear background was removed from the absorption plot. This background slope arises primarily from a frequency-dependent change in transmission in the fiber cell arrangement. Whilst the profile fits well to a Voigt profile, the Lorentzian linewidth component demonstrates that observable in-diffusion of air must have taken place during the fill process. A higher than expected total pressure of 8.5(3) kPa including a 1.7(1) kPa partial pressure of CO_2 is estimated from fitting the data to both the stronger R(30) profile and the weaker $^{13}C^{16}O_2$ P(14) line, taken in the same frequency scan. This estimated partial pressure of CO_2 is consistent with the target of 2 kPa in our 5-m cell. For this total pressure, the calculated peak absorption is 92 % with a HWHM of 0.010 cm^{-1} (≡ 300 MHz). Had there been no air ingress during the fill process, the peak linear absorption in a 5-m cell was expected to be 97 % with a calculated HWHM of 0.008 cm^{-1} (≡ 240 MHz). The linewidth with no air present is larger than the Doppler HWHM of 0.0047 cm^{-1} (≡ 140 MHz) because this line is close to saturation [Eq. (3)]. The effect of saturation also means that air present in the fiber has surprisingly little detrimental effect on the profile.

6. Frequency stability of the laser system

The experimental layout is shown in Fig. 2 and the final enclosed, compact, all-fiber laser stabilization system is shown in Fig. 4. The reference laser system and laser stabilization system both utilized Eblana fiber-coupled DFB butterfly mounted lasers [20]; both lasers came with Nufern PM1950 fiber pigtails. It is important to demonstrate our reported frequency stabilities using only sub-mW powers into the HCF, thereby maximizing the available usable output. The laser frequency stabilized using the CO_2-filled HCF had an additional semiconductor optical amplifier (SOA) to provide up to 16-mW fiber output. However, the SOA was not powered for the experimental results presented here to allow demonstration of the frequency stabilities required for this application at low powers, <1 mW. The lasers were supplied with integral isolators, but

Optics EXPRESS

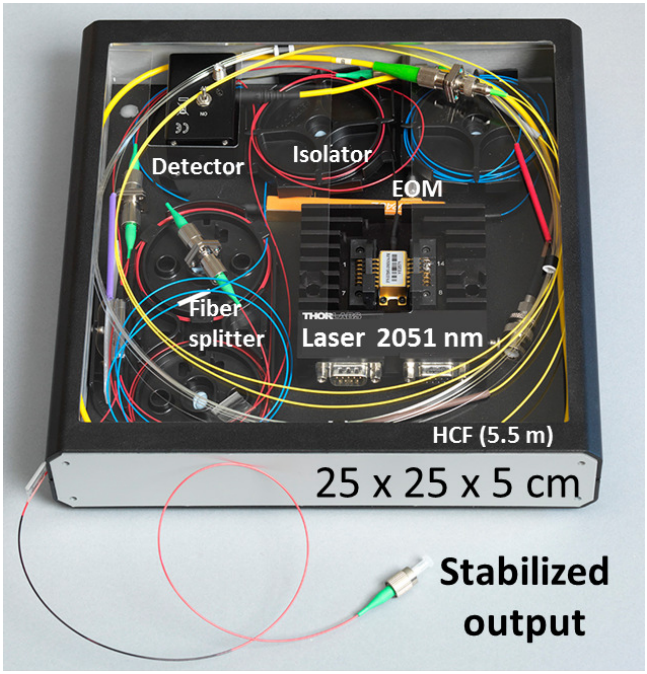

Fig. 4. The enclosed, compact, all-fiber system includes the laser module, fiber isolator, fiber splitter, fiber EOM, and fiber-coupled detector, as well as the Kagome HCF cell, which is coiled and held on an upper shelf in the enclosure of dimensions 25 x 25 x 5 cm.

an additional fiber-pigtail-based isolator stage was added after each DFB laser to further suppress any possible feedback from fiber interfaces. A 50:50 tap coupler (fiber splitter) was used to split the laser power between the stabilization system and the output, which in this case was used for beat frequency production. Both the splitter and fiber isolator pigtails were also made from Nufern PM1950. With this arrangement, the fiber path to the usable output comprised only one fiber type in order to minimize optical loss. The pigtailed EOM (used in the fiber path to the HCF) had a Corning PM1550 pigtail, but was otherwise optimized for use at 2051 nm and could be driven at frequencies up to a few GHz. This modulator was butt-coupled to the SMF28 pigtail of the HCF cell. A pigtailed InGaAs photo-detector with a 12-GHz bandwidth was connected to the output of the HCF.

The reference laser system used a conventional, commercially sourced 10-cm long free-space cell filled to a pressure of ~2.6 kPa. The output from a pigtailed laser was collimated and directed through this cell, with the transmitted beam detected using an InGaAs photo-detector with a specified response out to 2.6 μm. The laser was frequency modulated via the current input at a frequency of 17 kHz and a modulation depth on the order of 10 MHz peak to peak. The transmitted signal was detected using a phase sensitive detector, and the laser frequency was tuned to the R(30) line for stabilization. The SNR of this output was in the region of 1000 and so can be expected to be capable of demonstrating the key requirement for this application of a stability of 100 kHz at 10 s averaging time. As a check we also used two cells in series, doubling the absorption path length and observed no improvement in beat frequency stability. From these measurements, we therefore infer that the observed beat frequency stability primarily reflected the stability of the HCF-based device. The beat between the two lasers was observed using a free-space InGaAs photo detector (beats detector) of ~12 GHz bandwidth [Fig. 2]; this RF signal was amplified and sent to a frequency counter connected via a GPIB interface to a PC. The

Optics EXPRESS

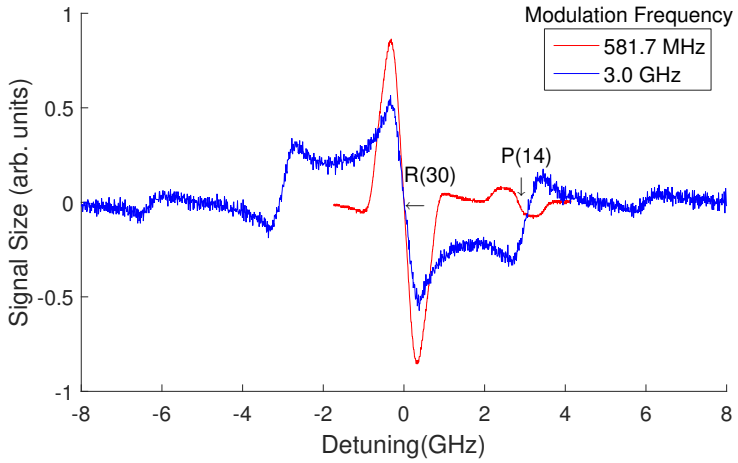

Fig. 5. PDH output spectrum at two modulation frequencies using a 2-kPa partial pressure Kagome HCF cell; produced by frequency tuning via the laser current. A 581.7 MHz modulation frequency allows us to lock either to the strong R(30) line or the weaker P(14) line in $^{13}C^{16}O_2$. The higher modulation frequency allowed us to investigate a novel way to lock the laser off resonance, here at ± 3 GHz (see text).

frequency stability of our HCF-based laser system was measured under various conditions. Firstly, the laser was locked to the R(30) transition using standard PDH laser stabilization techniques at various modulation frequencies [Fig. 5], using a 2-kPa partial pressure Kagome HCF gas cell, 5 m in length. We avoided the problems associated with counting a near-zero beat frequency by using a free-space acousto-optic modulator at 80 MHz in the reference laser system [Fig. 2]. The resulting beat varies around 80 MHz, as some frequency difference is expected between the free-space and fiber-cell systems, most likely due to the pressure and cell wall shifts, as well as error signal baseline offsets differing between the two systems. The measured frequency stability (Allan deviation) is shown in Fig. 6 using a 2-kPa HCF cell in the stabilization system and with the laser locked to R(30).

We observed some significant variability in the measured frequency stability and include in Fig. 6 beat frequency data with an instability of only 2 kHz at 10 s, as well as more typical stability data (~40 kHz at 1 s). The beat frequency stability was found to be dependent on a number of electronic and environmental parameters. Temperature and pressure fluctuations could affect the compact fiber laser system and the reference systems differently, causing a drift in the beat frequency over time. The fused joints in the Kagome HCF gas cell were extremely sensitive to both temperature changes and any physical manipulation or vibrations. The frequency stability of the system was improved by placing first the fiber cell and finally the entire fiber and laser system into an enclosure. The final compact package, including the laser, detector, fibers and HCF gas cell, was completely enclosed in the compact 25 x 25 x 5 cm box as shown in Fig. 4. We observed variations in the PDH lock baseline over time, which directly affected the beat frequency measured. This could be due mainly to modal interference in the Kagome HCF itself, which is frequency dependent. To mitigate this effect, the modulation frequencies we worked at were chosen specifically to minimize the baseline excursions with respect to small changes to the modulation frequency, and the stability at these frequencies was found to be repeatable as long as the fiber gas cell was not physically adjusted. On faster timescales, optical feedback to the DFB laser could have been affecting the stability of the laser for that system. The best system stability corresponded to the most stable lab environmental conditions (e.g. data acquired

Optics EXPRESS

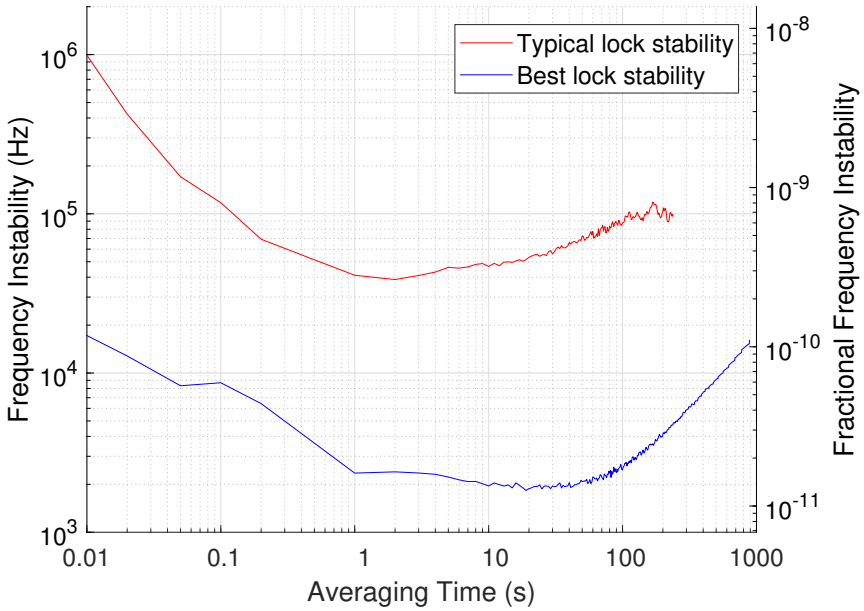

Fig. 6. Frequency stability (Allan deviation) and related fractional frequency instability of a 2051-nm (146-THz) laser stabilized to a 5-m-long Kagome HCF cell with a partial pressure of 2 kPa of CO_2. For these results, a zero dead-time counter was used (Stanford SR620) for the short gate time results (≤1 s), and an Agilent 53181A for gate times 1 s and longer.

overnight), which had a knock-on effect of reducing the frequency deviations of both systems on all timescales.

The long-term stability of the frequency reference for a space-based system is also an important requirement. Repeated beat-frequency measurements with the HCF system stabilized to the R(30) line showed frequency reproducibility of 0.4 MHz (one standard deviation) for beat frequency measurements with a weighted mean of ~91 MHz for data taken over a timescale of > 1 month, as shown in Fig. 7. The reference system and stabilization system lasers, their control electronics, and the rf signal to the EOM were turned off between measurements, with the systems given at least 5 minutes to warm up upon restart before each subsequent beat measurement was begun.

In addition to locking a laser to the line center of the R(30) transition, it is necessary to be able to tune and ideally lock the laser off-resonance, typically ~3 GHz from line center, for the differential measurements required in DIAL. We explored two ways of achieving this and the results are shown in Fig. 8. In the first method, the 2-kPa HCF cell was used to lock the laser to the weak P(14) transition of the $^{13}C^{16}O_2$ isotopologue. The resulting beat frequency was 2.78 GHz and the frequency stability (Allan deviation) is shown in Fig. 8. The reduction in measured frequency stability when locking to the weaker P(14) transition compared to the R(30) feature is due to the difference in signal amplitude between the two transitions, which translates directly to PDH lock signal size. A second method to achieve this ~3 GHz offset, without needing to access another transition, is to employ PDH spectroscopy, but modulate the laser at ~3 GHz. In this arrangement, the laser can be locked to one of the two subsidiary electronics zero crossings of the PDH signal, either ~3 GHz higher or lower in frequency, see Fig. 5. This method uses a single error signal to produce both the on-resonance and off-resonance lock points, and enables the off-resonance lock point to be tunable in frequency. The resulting frequency stability of this method is also shown in Fig. 8. The frequency stability measured is reduced compared to locking

Optics EXPRESS

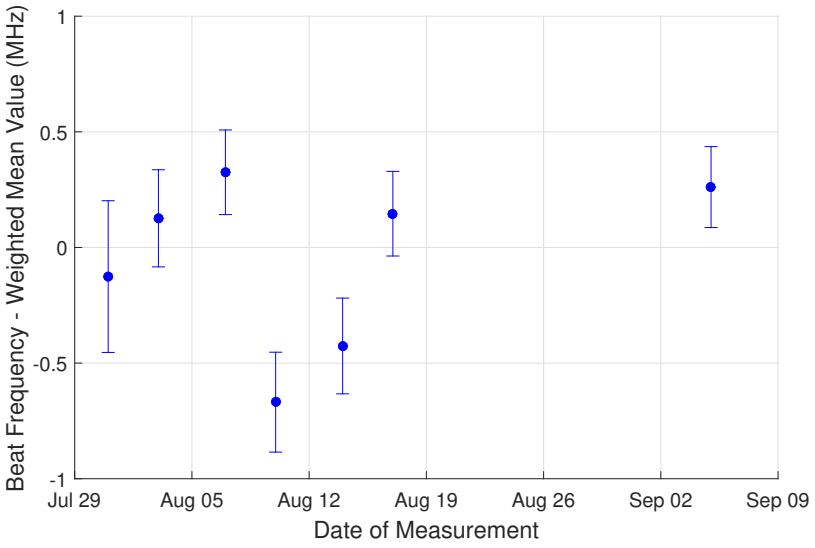

Fig. 7. Reproducibility of the laser locked to component R(30); each data point is the mean of between 4200 and 14700 one-second gate time beat frequency measurements. The weighted mean of the complete data set (~91 MHz) has been subtracted from each beat frequency value. The data were taken over a period of more than a month and the results show a reproducibility (expressed as a standard deviation) of 0.4 MHz.

to the zero crossing at the lower modulation frequency, which is due to the SNR reduction, as can be seen in Fig. 5, reflecting the technical difficulty in achieving as high a modulation index at frequencies greater than 1 GHz. Frequency stability results from the two off-resonant locking methods diverge over longer timescales due to a change in the drift characteristics of the reference and stabilized laser systems at the times when the two data sets were taken. Using this second locking arrangement we have also demonstrated that it is possible to tune the lock point by changing the modulation frequency. This method is valid for modulation frequencies higher than ~1.5 GHz, which is the frequency value at which the PDH signal sidebands are resolved from the central feature, due to the linewidth of the R(30) absorption line.

7. Conclusion

We have presented the results of a study of a compact Kagome HCF-based CO_2-stabilized laser at 2051 nm. We have shown that, once filled, the linear absorption through the gas cell remains stable over a period of at least one year, even though there was some in-diffusion of air at the time of the initial fill. We find that it is better to aim for a higher concentration of CO_2 (i.e. 2 kPa rather than 0.1 kPa in a 5-m fiber), as this optimizes the SNR profile of the locking signal, with maximum absorption but minimal line broadening. By aiming for a partial pressure giving over 90 % absorption, i.e. close to saturation; $A \gg 1$ in Eq. (3), the profile is more tolerant of air ingress at the time of the fill, even though the linewidth becomes larger and the profile more flat-topped as saturation is approached.

We explored two methods of providing a frequency lock ~3 GHz from line center for DIAL applications. In one configuration, we locked to the weak P(14) line in $^{13}C^{16}O_2$ and in a second approach we locked to a subsidiary zero crossing of the PDH signal when applying a ~3 GHz modulation frequency. In our setup, this method was limited by the EOM not being able to provide the optimum modulation index at this frequency. We demonstrated similar frequency

Optics EXPRESS

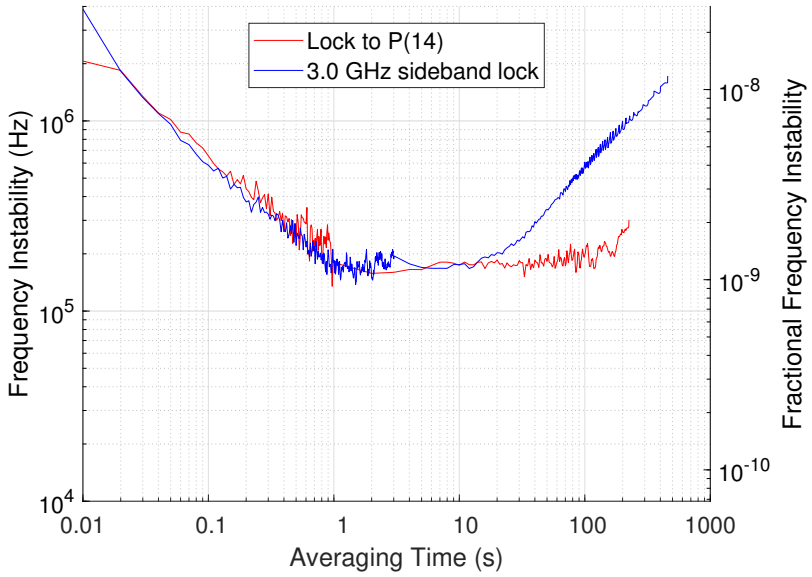

Fig. 8. Frequency stability (Allan deviation) and related fractional frequency instability of a 2051-nm (146-THz) laser stabilized to a 5-m-long Kagome HCF cell with a partial pressure of 2 kPa of CO_2, locked to the weak transition ~2.7 GHz away (red trace), and to the PDH ~3 GHz sideband (blue trace). An Agilent 53181A counter was used the measure the beat frequency between this laser and a reference laser. For short gate times (<1 s) the results were taken by averaging data observed using a 10-ms gate although this results in a significant dead time in the measurement at timescales <1 s.

stability up to 10-s timescales using both techniques and conclude that improved results could be obtained with longer fiber cells (e.g. 10 - 15 m) filled to higher pressure (8 kPa).

In conclusion, for a laser stabilized to the line center of the strong R(30) transition, the frequency stability of our laser system is typically better than 40 kHz at 1 s, with a frequency reproducibility of 0.4 MHz for data taken over a timescale of > 1 month. Additionally the Kagome HCF cells have been shown to maintain the same concentration of CO_2 on timescales exceeding 1 year, implying devices using them will not be limited by gas cell lifetime. Finally we have shown that the Kagome-HCF-cell-based laser system can also be stabilized at frequencies far offset (~ 3 GHz) from line center. These results exceed the requirements for a reference system for CO_2 environmental monitoring from space using DIAL.

Funding

European Space Agency (ESA) under ESA Contract No. 4000107487/13/NL/PA.

Acknowledgments

The authors would like to thank J. P. Wooler for major contributions to the cell fabrication process and Mohsin Haji and Helen Margolis for their careful reading of the manuscript.

Disclosures

The authors declare that there are no conflicts of interest related to this article.